

Final Report of deformation behavior of hexagonal

Tianyi Wang, Zhicheng Ren

Abstract—This report presents the development and implementation of a numerical simulation to study the deformation behavior of hexagonal lattice structures under external loads. The dynamic time step method was used to model the mechanical response of the structure. It includes the generation of hexagonal lattice geometry, the definition of mechanical properties, the establishment of motion equations, and the realization of numerical solutions. We hope to learn the mechanical properties and contribute to the design of elastic materials.

I. INTRODUCTION

Hexagonal lattice structures are widely used in various engineering applications due to their high strength-to-weight ratio and efficient material distribution[1]. Understanding the mechanical behavior of such structures under external loads is critical for designing elastic and lightweight materials, especially in the aerospace, mechanical and civil engineering fields.

In this project, the goal is to study the deformation of hexagonal lattice structures. Due to its unique mechanical properties and excellent energy absorption capacity, hexagonal lattices not only have high strength and ductility, but also exhibit excellent impact resistance in complex dynamic environments[2], providing an ideal model for the design of high-performance elastic materials.

In this study, the deformation behavior of hexagonal lattice structures under applied loads is studied from the perspective of engineering. We simplified the structural model to a hexagonal frame. The deformation characteristics of hexagonal lattice structures under load are studied by computer simulation. We wrote a help function that allows us to arbitrarily set the number of 6-sided shapes for the entire model. By simulating and analyzing the deformation characteristics of hexagonal lattice structures under load conditions, we hope to understand the mechanical properties of hexagonal lattice structures and contribute to the design of advanced elastic materials[3].

II. MODEL SETUP

generate_rods:

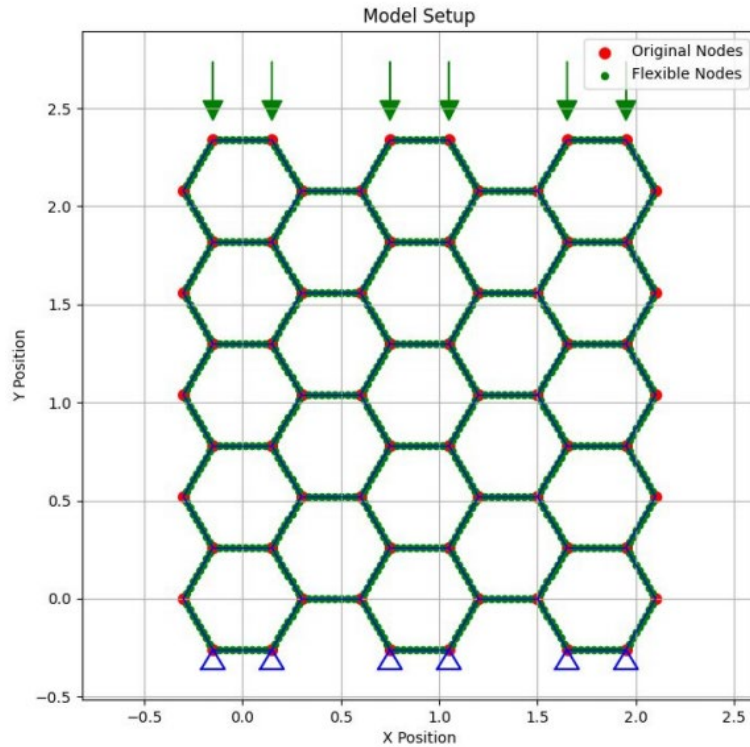
```
rods_dict = {idx: rod for idx, rod in enumerate(rods)}
rods_idx = {rod: idx for idx, rod in enumerate(rods)}
while error > tol:
    f = m / dt * ((q_new - q_old) / dt - u_old)
    J = mMat / dt ** 2
    for rod in rods_dict:
        s_flexible = list(range((2*npoint + 2*rod*nv_rod), (2*npoint +
2*(rod+1)*nv_rod)))
        s1 = [2*rods_dict[rod][0], 2*rods_dict[rod][0]+1] + s_flexible +
[2*rods_dict[rod][1], 2*rods_dict[rod][1]+1]
        q_new_local = q_new[s1]
        Fb, Jb = getFb(q_new_local, EI, deltaL)
        Fs, Js = getFs(q_new_local, EA, deltaL)
        f[s1] = f[s1] - (Fb + Fs + W[s1])
        J[np.ix_(s1, s1)] = J[np.ix_(s1, s1)] - (Jb + Js)
```

generate_hexagonal_nodes:

```
for nodes in curvature_dict:
    main_node = nodes[0]
    s_main = [2 * main_node, 2 * main_node + 1]
    if main_node < nodes[1]:
        s_neighbour1_x = 2 * npoint + 2 * rods_idx[(main_node, nodes[1])] * nv_rod
        s_neighbour2_x = 2 * npoint + 2 * rods_idx[(main_node, nodes[2])] * nv_rod
    elif nodes[1] < main_node < nodes[2]:
        s_neighbour1_x = 2 * npoint + 2 * (rods_idx[(nodes[1], main_node)] + 1) *
nv_rod - 2
        s_neighbour2_x = 2 * npoint + 2 * rods_idx[(main_node, nodes[2])] * nv_rod
    else:
        s_neighbour1_x = 2 * npoint + 2 * (rods_idx[(nodes[1], main_node)] + 1) *
nv_rod - 2
        s_neighbour2_x = 2 * npoint + 2 * (rods_idx[(nodes[2], main_node)] + 1) *
nv_rod - 2
    s_neighbour1 = [s_neighbour1_x, s_neighbour1_x + 1]
    s_neighbour2 = [s_neighbour2_x, s_neighbour2_x + 1]
    xk, yk = q_new[s_main]
    xkm1, ykm1 = q_new[s_neighbour1]
    xkp1, ykp1 = q_new[s_neighbour2]
    s2 = s_neighbour1 + s_main + s_neighbour
```

generate_flexible_nodes:

```
geb, flag1 = gradEb(xkm1, ykm1, xk, yk, xkp1, ykp1, curvature_dict[nodes], deltaL, EI)
if flag1 == -1:
    print(nodes)
    print(curvature_dict[nodes])
    break
f[s2] += geb
J[np.ix_(s2, s2)] += hessEb(xkm1, ykm1, xk, yk, xkp1, ykp1,
curvature_dict[nodes], deltaL, EI) # Size is 6x6
f_free = f[free_index]
J_free = J[np.ix_(free_index, free_index)]
dq_free = np.linalg.solve(J_free, f_free)
q_new[free_index] = q_new[free_index] - dq_free
error = np.linalg.norm(f_free)
iter_count += 1
if iter_count > maximum_iter:
    flag = -1
    print("Maximum number of iterations reached.")
    print(error)
    return q_new, flag
```



calculate_curvature:

```

node0 = np.array([xkm1, ykm1, 0.0])
node1 = np.array([xk, yk, 0])
node2 = np.array([xkp1, ykp1, 0])
m2e = np.array([0, 0, 1])
m2f = np.array([0, 0, 1])
kappaBar = curvature0
gradKappa = np.zeros(6)
ee = node1 - node0
ef = node2 - node1
norm_e = np.linalg.norm(ee)
norm_f = np.linalg.norm(ef)
te = ee / norm_e
tf = ef / norm_f
flag1 = 1
chi = 1.0 + np.dot(te, tf)
if abs(chi) < 1e-10:  # Add small threshold
    flag1 = -1
    chi = 1e-10  # Prevent division by zero
kb = 2.0 * np.cross(te, tf) / chi
tilde_t = (te + tf) / chi
tilde_d2 = (m2e + m2f) / chi
kappa1 = kb[2]

```

III. SIMULATION RESULT

Figure 1 below is the initial state of the simulation(8 hexagon).

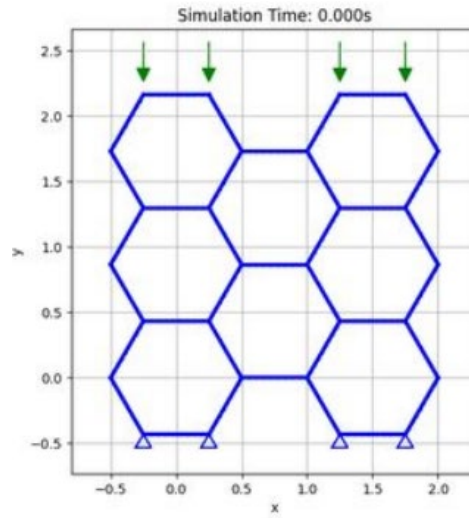


Fig. 1 Initial state of the simulation(8 hexagon)

Figure 2 below is the initial state of the simulation(23 hexagon).

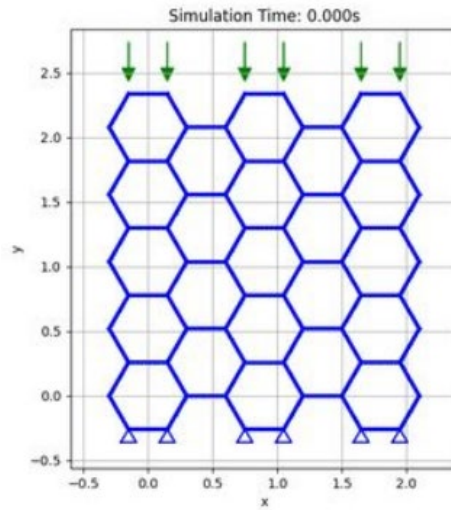


Fig. 2 Initial state of the simulation(23 hexagon)

Figure 3 below is the initial state of the simulation(46 hexagon).

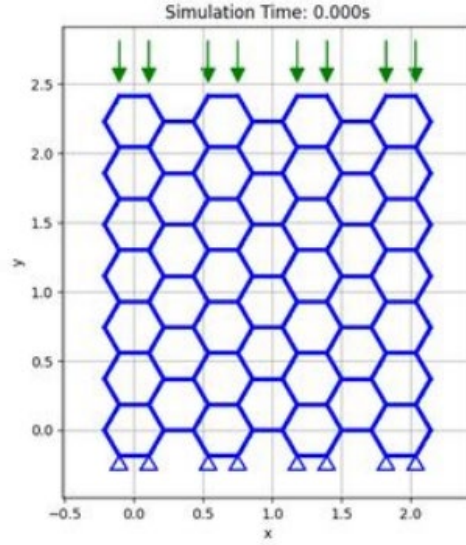


Fig. 3 Initial state of the simulation(46 hexagon)

The simulation generates a hexagonal lattice structure composed of rods. All rods have the same physical properties. These rods connect nodes to form the overall structure, while there are also rods that connect the vertices of hexagons to the centers of adjacent units, enhancing the structural network. The length of each rod is 0.5 meters. The structure is subject to gravity and additional downward loads, and nodes at the bottom are fixed to simulate anchoring conditions.

On this basis, we set the boundary conditions of the whole model in detail: First, the fixed constraints are imposed on the four key points at the bottom of the model to ensure that the four support points will not have any displacement or rotation during the calculation process, so as to provide a stable base plane for the force analysis of the superstructure. This fixation can be understood as a constraint on all degrees of freedom in the region, aiming to simulate the role of the foundation or the bearing base in real engineering. At the same time, in the upper part of the model, downward vertical concentrated loads or distributed loads are applied in the upper left and upper right corners respectively to simulate the deformation characteristics and stress transfer process of the structure under stress.

The final state of the simulation (8 hexagon) is shown below:

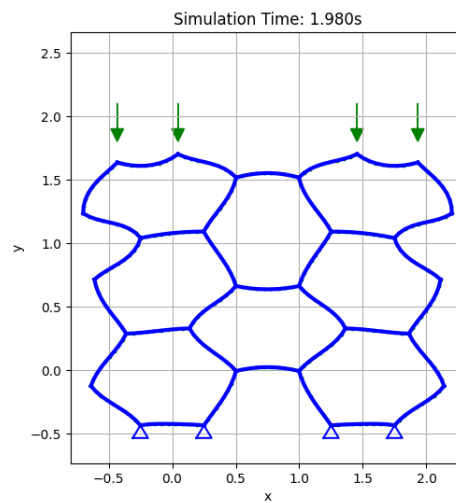


Fig. 4 Final state of the simulation(8 hexagon)

The final state of the simulation (23 hexagon) is shown below:

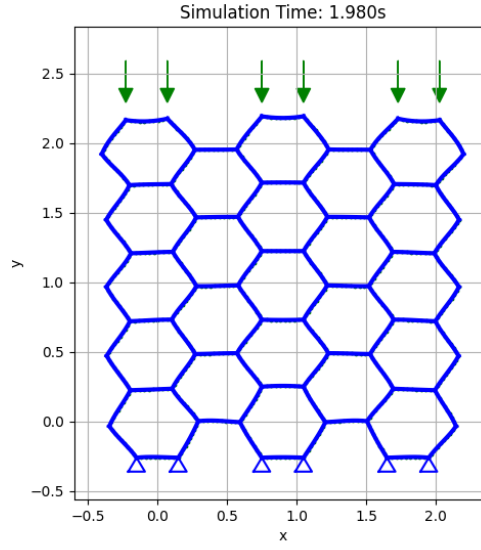


Fig. 5 Final state of the simulation(23 hexagon)

The final state of the simulation (46 hexagon) is shown below:

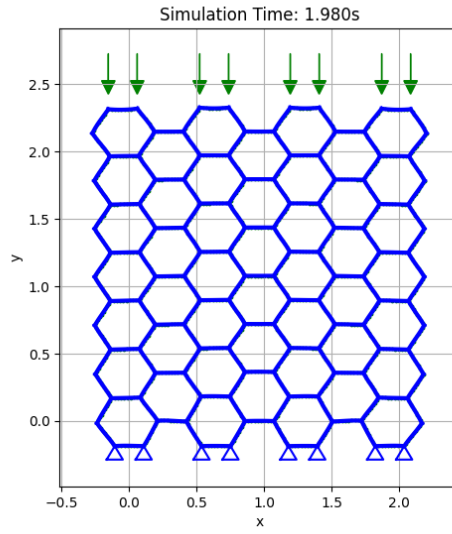


Fig. 6 Final state of the simulation(46 hexagon)

In this simulation, the time interval is 0.06 seconds and $\Delta t = 0.005s$. The mechanical model of bending and axial deformation is calculated as follows:

Curvature at node k is:

$$K = 2 \tan\left(\frac{\theta_k}{2}\right) / l_k \quad (1.1)$$

Simple geometry:

$$R_k = \frac{dl}{2 \tan(\phi_k / 2)} \quad (1.2)$$

$$\phi_k = \tan^{-1} \frac{(e^{k-1} \times e^k) \cdot \hat{e}_z}{e^{k-1} \cdot e^k} \quad (1.3)$$

For naturally curved beam:

$$E_b = \sum_{k=2}^{N-1} E_{b,k} \quad (1.4)$$

where $E_{b,k} = \frac{1}{2} \frac{EI}{dl} (K_k - K_k^0)^2$, $K_k = 2 \tan(\phi_k / 2)$

Total elastic stretching energy:

$$E_s = \sum_{k=1}^{N-1} E_s^k \quad (1.5)$$

Stretching energy per edge:

$$E_s^k = \frac{1}{2} EA \varepsilon^2 dl \quad (1.6)$$

Axial stretch:

$$\varepsilon = 1 - \frac{\sqrt{(x_{k+1} - x_k)^2 + (y_{k+1} - y_k)^2}}{dl} \quad (1.7)$$

IV. Conclusion

The algorithms and solution processes presented in this report focus on nonlinear finite element analysis of the equilibrium state of flexible member structures under external loads. By modeling and solving the bending and stretching deformation modes of the member, the solver can iteratively calculate the equilibrium state of the structure under the premise of given materials, geometric parameters and constraints.

In this method, the "residual force" is used as the convergence criterion, that is, the internal element force and stiffness characteristics are obtained on the basis of the assumed displacement field of the bar. After balancing with the external load, if the residual force is less than the convergence threshold, the stable equilibrium can be considered.

As part of nonlinear finite element analysis, tensile stiffness and internal force are determined by the variation of element length. When the element is stretched or compressed by external forces, the internal force and stiffness change accordingly. By comparing the change of displacement with the reference length, the tensile strain and stress can be calculated to obtain the tensile internal force of the element and its influence on the stiffness of the system.

The bending stiffness is related to the deviation between the internal force and the element curvature. The gradient and second derivative of the bending strain energy with respect to degrees of freedom can be calculated by evaluating the curvature change of the member at the joint joint and the target curvature. In this way, the internal forces caused by the bending and the contribution to the stiffness matrix can be precisely included.

On this basis, the solver solves with external loads and boundary conditions by assembling the force and stiffness of each element into the global equation. If geometric or numerical degradation occurs during iteration, the program flags and prompts to identify possible problem areas.

The results show that the method can reliably predict the steady-state equilibrium shape, internal force distribution and stress-strain state of flexible member under complex load and nonlinear deformation conditions. This provides a reliable and efficient numerical method for further structural optimization design, mechanical property evaluation and engineering application.

REFERENCES

- [1] Aminanda, Y., B. Castanié, J.J. Barrau, et al. "Experimental Analysis and Modeling of the Crushing of Honeycomb Cores." *Applied Composite Materials*, vol. 12, 2005, pp. 213–227.
- [2] Asprone, Domenico, et al. "Statistical Finite Element Analysis of the Buckling Behavior of Honeycomb Structures." *Composite Structures*, vol. 105, Nov. 2013, pp. 240–255.
- [3] Mousanezhad, D., S. Babaei, H. Ebrahimi, et al. "Hierarchical Honeycomb Auxetic Metamaterials." *Scientific Reports*, vol. 5, 2016, article 18306. Nature, <https://doi.org/10.1038/srep18306>.
- [4] Partovi Meran, Ahmad, et al. "Numerical and Experimental Study of Crashworthiness Parameters of Honeycomb Structures." *Thin-Walled Structures*, vol. 78, May 2014, pp. 87–94.
- [5] Papka, S.D., and S. Kyriakides. "Experiments and Full-Scale Numerical Simulations of In-Plane Crushing of a Honeycomb." *Acta Materialia*, vol. 46, no. 8, 1 May 1998, pp. 2765–2776.
- [6] Qi, Chang, et al. "Advanced Honeycomb Designs for Improving Mechanical Properties: A Review." *Composites Part B: Engineering*, vol. 227, 15 Dec. 2021, article 109393.
- [7] Yamashita, M., and M. Gotoh. "Impact Behavior of Honeycomb Structures with Various Cell Specifications—Numerical Simulation and Experiment." *International Journal of Impact Engineering*, vol. 32, nos. 1–4, Dec. 2005, pp. 618–630.
- [8] Qi, Chang, et al. "Mechanical Properties of a Honeycomb Structure Dispersed with 3D Graphene." *ACS Omega*, vol. 9, no. 5, 2024, pp. 1234–1245. DOI: 10.1021/acsomega.3c10138.
- [9] Venkateswaran, A., et al. "Crashworthiness of Ultrathin Aluminum Honeycomb Structures." *Mechanics of Solids*, vol. 59, no. 3, 2024, pp. 240–256. DOI: 10.1134/S0025654424603550.
- [10] Zhang, Hong, et al. "Innovative Design and Equivalent Mechanical Properties of a New Combined Honeycomb Structure." *Mechanics of Composite Materials*, vol. 58, no. 2, 2022, pp. 315–326. DOI: 10.1007/s10778-022-01161-2.